ATLAS Internal Note
INDET-NO-203
5 March 1998

Yearly operation profile of the ATLAS SCT detectors

25 January, 1998 T. Kondo, KEK

Abstract

A numerical prediction of the operation of the ATLAS barrel silicon microstrip detector is done with three scenarios of applied voltage on the detector. These scenarios approximately correspond to the operation of p-on-n and n-on-n detectors. Various operational parameters are examined to see the effective operation period of the system.

1. Input parameters.

1.1 Fluence

The neutron equivalent fluence listed in ATLAS ID-TDR p.394 is used [1]. Low luminosity operation at $10^{33}cm^{-2}s^{-1}$ is assumed for the first three years, then operation at $L=10^{34}$ $cm^{-2}s^{-1}$ follows in subsequent years. Total fluxes for initial ten years are listed in Table 1.

Fig.1 shows the integrated fluence as a function of operating year.

Table 1 Integrated fluence

Radius [mm]	Integrated Fluence [n_{eq}/cm^2]
300	1.30×10^{14}
373	1.03×10^{14}
447	0.85×10^{14}
520	0.77×10^{14}

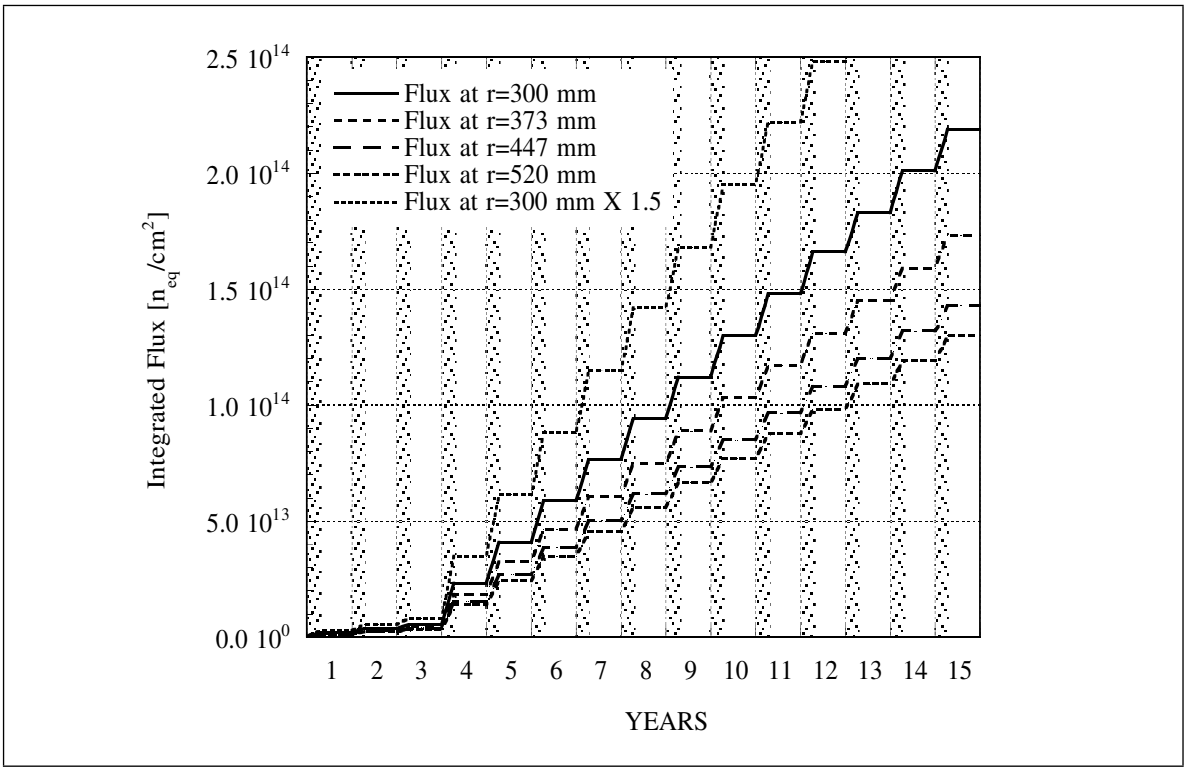

Figure 1 Integrated neutron equivalent fluence [1]. 50% more case (×1.5 fluence) is shown for r=300 mm. Shade indicates operation periods.

1.2 Access scenario

The temperature of the detector plays an important role. It is assumed to approximately follows the standard access scenario (SAP) proposed in the TDR [1]:

Number of days	100	100	2	14	149	days
Detector status	operation	off	access	maintenance	off	
Temperature of detector	~ -7	- 7	+ 20	+ 17	- 7	˚C

1.3 Detector annealing parameters

Parameters for the long term behavior of the silicon detector are taken from the TDR Table 11-5 (p 402) [1,2]. Although the short term beneficial annealing is neglected in TDR, it is maintained in the present calculation since its effect on the depletion voltage is not negligible during the period of detector operation [3]. The formula used for the change of depletion voltage are

$$V(dep) = \frac{e \cdot d^2 \cdot |N_{eff}|}{2\varepsilon'\varepsilon_0},$$

$$N_{eff} = N_{eff\,0} - N_{C0}(1 - e^{-c\Phi}) - g_S e^{-t/\tau(T)} - g_C\Phi - g_Y\Phi\left(1 - \frac{1}{1 + k_0 \exp(-E_a/k_B T) \cdot g_Y \Phi \cdot t}\right),$$

$$\tau(T) = \tau_0 \exp(-0.175 \cdot T[^\circ C]),$$

where $N_{eff0} = 5 \times 10^{11}/cm^3$, $\varepsilon' = 11.6$,

$N_{C0} = 1.96 \times 10^{11}/cm^3$, $c = 2.29 \times 10^{-13} cm^2$,

$g_S = 0.0193/cm$, $g_C = 0.046/cm$,

$\tau_0 = 70$ day, $g_Y = 0.0177/cm$,

$k_0 = 520 cm^3 s^{-1}$, $E_a = 1.31$ eV,

T is the detector temperature, d is the detector thickness, t is the elapsed time, and Φ is the integrated neutron-equivalent fluence.

1.4 Bulk leak current

C. Buttar and J. Carter [4] recently measured the bulk leakage current of both p-in-n and n-in-n detectors irradiated to 3 x10^{14} protons/cm^2, which approximately corresponds to 2 x10^{14} n_{eq}/cm^2 ;

V(apply)	300	400	500	V
I(leak) at 0˚C	1346	1507	1777	µA

Figure 2 show the data and its polynomial fit which is used in the calculation. The current is assumed to be proportional to the integrated fluence Φ. The actual leakage current depends on the detector temperature;

$$i \propto T^2 \exp(-E_g/2k_B T),$$

where E_g is set to 1.23 eV.

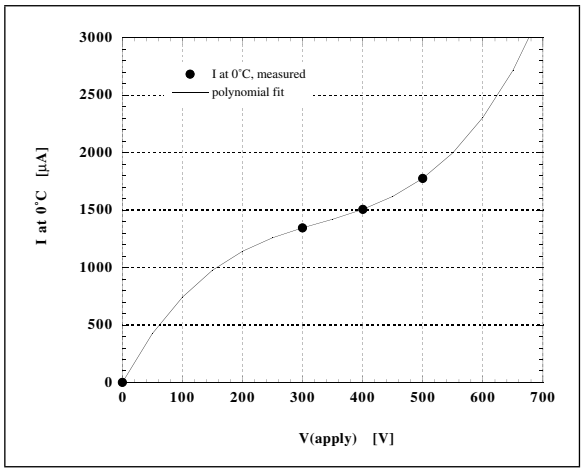

Figure 2 Bulk leakage current as a function of applied voltage for irradiated detector of 62 x 62 x 0.3 mm^2. The solid line if a polynomial fit.

1.5 Module model

Two designs of the ATLAS barrel module are employed to estimate the thermal property. The difference of the design is the shape of the TPG baseboard as shown in Figure 3 and Figure 4.

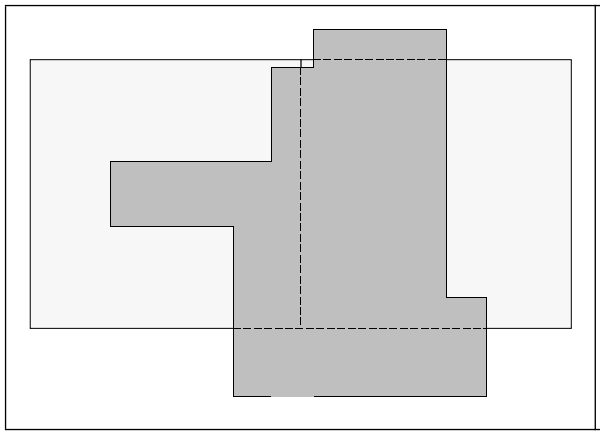

Figure 3 Design of the barrel module type “nose”. Dark shaded area indicates the TPG baseboard.

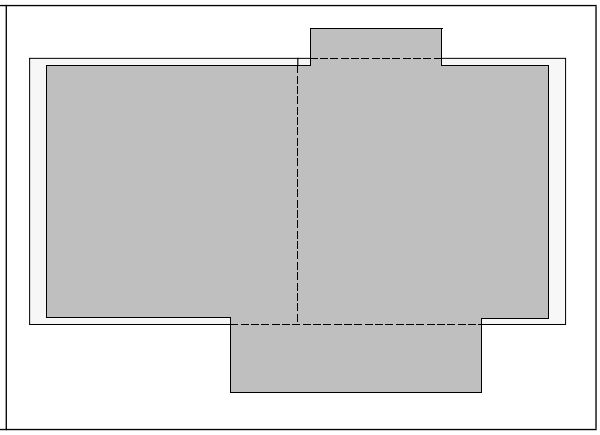

Figure 4 Design of the barrel module type “cover-all”.

1.6 Thermal simulation

A thermal simulation using ANSYS 5.1 was done for these module designs. The temperature constraint is imposed at the contact area between module and cooling pipe which is running along the module side. Neither convection nor radiation from/to the surface of the detector is included in the thermal simulation since these effects are small. Two temperature constraints T(cool) = -10˚C and -15˚C are tried. Note that the actual coolant temperature is about 3˚C below these contact temperatures due to thermal resistance.

The simulation is done as a function of normalized bulk heat generation $q(Si)_0$ at 0˚C. Figure 5 shows the temperature of the top-left corner of the module where thermal runaway starts up. The solid lines in the figures are polynomial fits, which are used in the subsequent calculation.

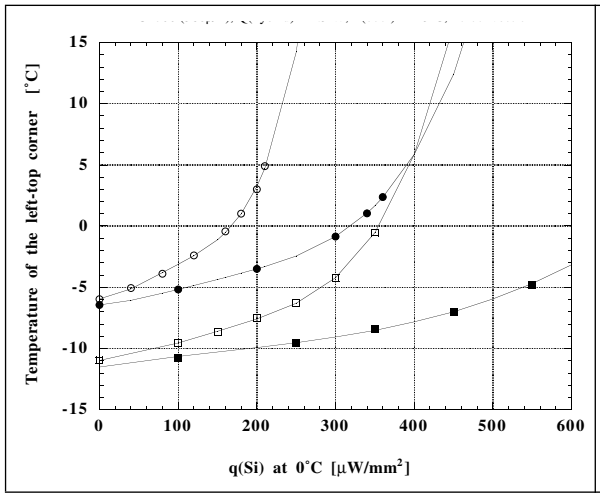

Figure 5 Temperature of the left-top corner of the detector as a function of $q(Si)_0$ (bulk heat generation normalized at 0˚C) and its polynomial fit.

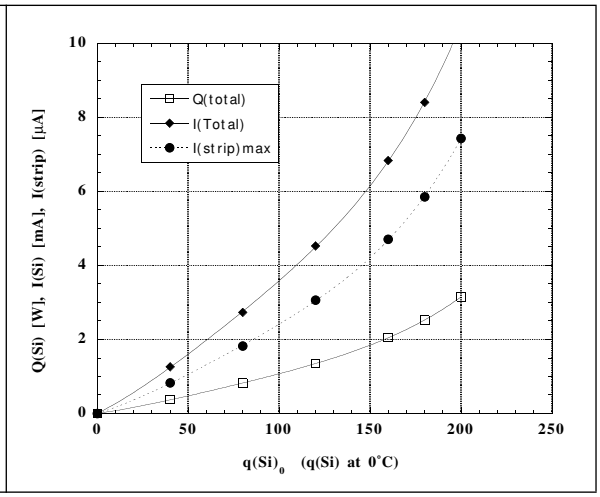

Figure 6 Q(Si): total bulk heat in [W], I(Si): total bulk current in [mA], I(strip) max. strip current in [μA] at T(cool)=-10˚C.

2. Scenarios of the applied voltage

In order to calculate the yearly performance of the detector, one has to determine the strategy of the applied voltage on silicon detectors. Three cases are assumed;

case-A: $V(apply) \geq V(dep)$,

case-B (p-on-n): $V(apply) = V(dep) + 100$ V ,

case-C (n-on-n): $V(apply) \geq V(dep)$ but $V(apply) \leq 300$ V ,

where V(dep) is the predicted depletion voltage at the end of each yearly operation period. The applied voltage V(apply) is kept constant throughout each operation. When V(dep) is less than 100V, the minimum applied voltage is set to 100 V for all scenarios. The

Case-B approximately corresponds to the voltage scenario for the p-on-n detectors, while case-C may be close to that for n-on-n detectors. Additional 100 V in the case-B includes possible spread of depletion voltage prediction of irradiated detectors. The limit 300 V is chosen for case-C conservatively for safe operation [5].

3. Calculation

The present numerical calculation is done in following way;

1. Calculate the integrated fluence Φ as a function of operating year.
2. Calculate the depletion voltage V(dep) by taking the time dependence of the detector temperature into account.
3. Set the applied voltage V(apply) according to the rules for each scenario. The predicted V(dep) at the end of the coming run is used in determining the applied voltage.
4. Estimate the bulk leak current at 0˚C using the polynomial fit to the measured voltage dependence of the leak current (see Section 1.4). Then the bulk heat generation $q(Si)_0$ at 0˚C is calculated by multiplying the applied voltage and the leak current.
5. The various operational parameters, temperature T, total bulk heat, total bulk current and maximum strip current, are calculated from the value of $q(Si)_0$ using the polynomial fits to the thermal simulation results (see Section 1.6).

4. Yearly profiles and detector life

4.1 Depletion voltage

shows the summary of predicted depletion voltage for the cases of nominal and 1.5 X fluence and also for both -10˚C and -15˚C. One sees there is little dependence on cooling contact temperature T(cool), while both fluence and radius dependences are quite large.

The reason of small T(cool) dependence can be understood that T-dependent anti-annealing effect are small during detector operation as shown in Figure 7. One can clearly see that most of the anti-annealing effects comes from the access period (2 days at 20˚C and 14 days at

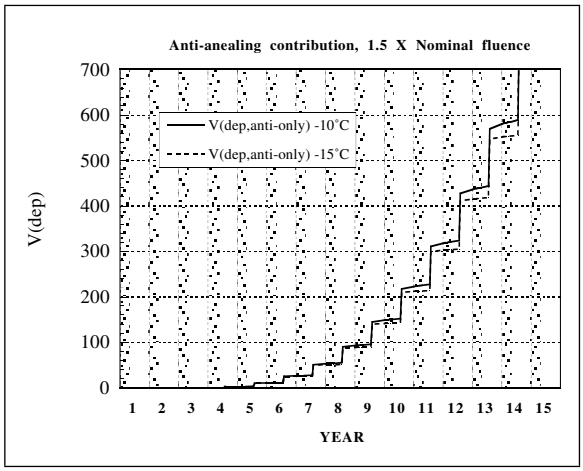

Figure 7 Depletion voltage due to the anti-annealing term for-10˚C and -15˚C at 1.5 X flux and r=300 mm. Shaded area corresponds to detector operation.

17˚C)

In the calculation of the depletion voltage, the second-order effect of operating detector temperature, namely non-uniform temperature distribution over silicon detector may create non-uniform depletion voltage. But it turned out small (less than 10 V) as long as detector temperature are near or below -5˚C. This is consistent with the observation shown in Figure 7.

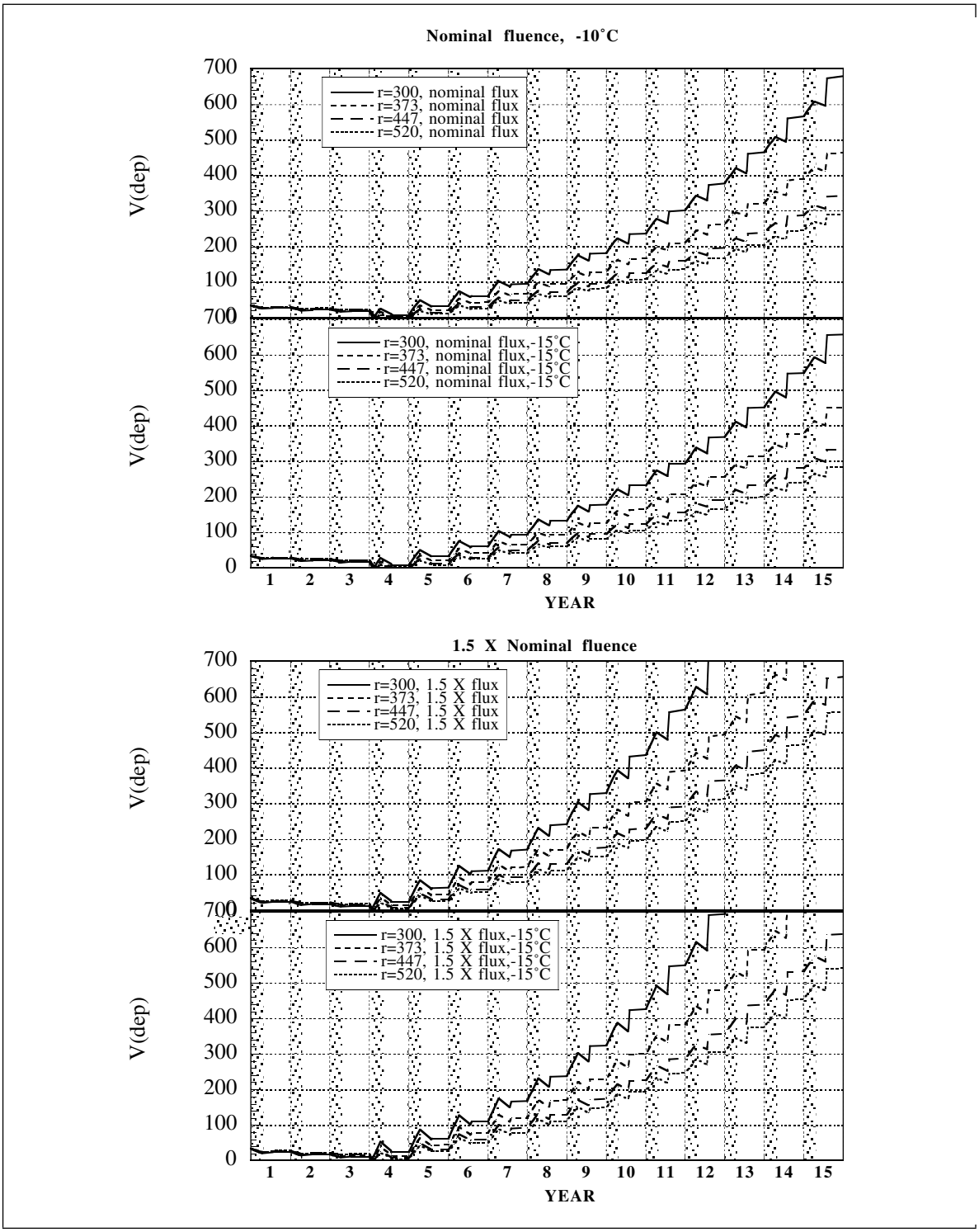

Figure 8 Predicted depletion voltages V(dep) at various radii and for nominal fluence (top 2 graphs) and 1.5 X fluence (bottom 2 graphs). 1st and 3rd graphs are for T(cool)=-10˚C while 2nd and 4th for -15˚C.

4.2 Applied voltage

Now the depletion voltage is known as a function of year, the applied voltage is determined according to the scenario described in Section 2. For cases A and B, the applied voltage is always above V(dep) to get good charge collection efficiency, but the limit may comes from the maximum operating voltage, for example 500 V.

In Case-C in which V(apply) is ≤ 300V, the applied voltage eventually becomes lower than V(dep) in later years. Figure 9 plots the ratio R_V = V(apply) / V(dep) at various radii for two fluence case. The proposed n-on-n detector still works below V(dep) but one has to watch this ratio carefully.

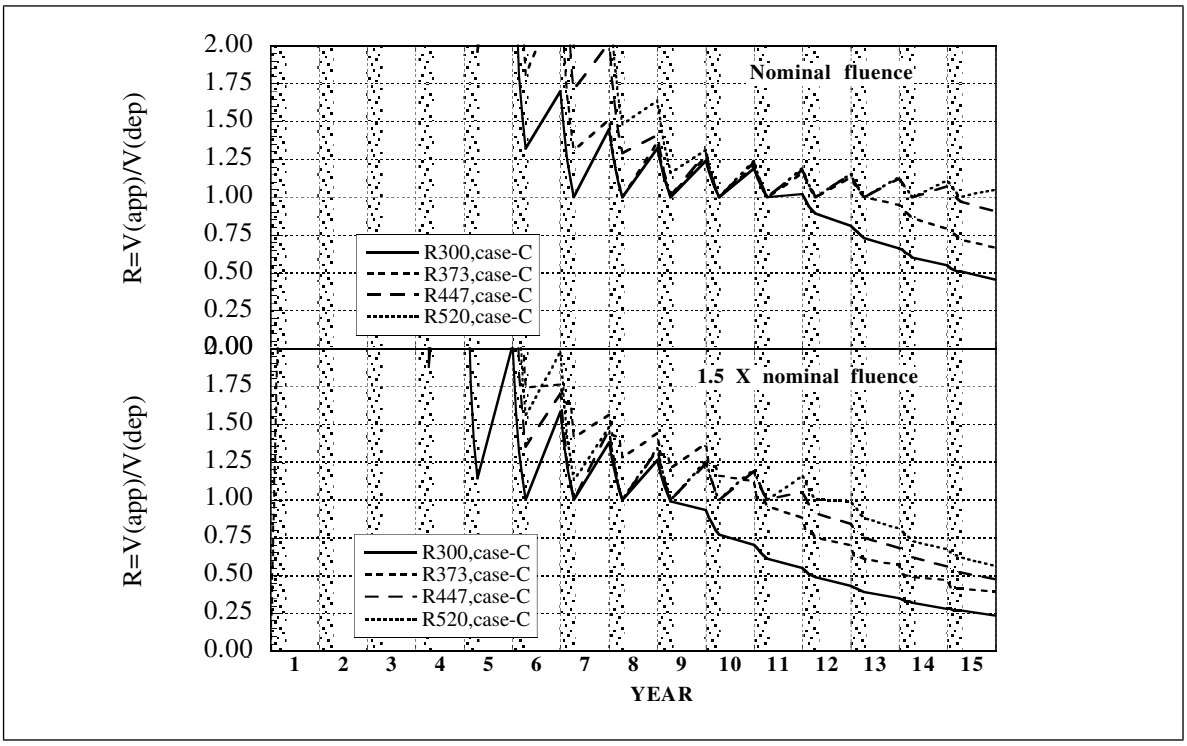

Figure 9 The voltage ratio R_V=V(apply)/V(dep) for the case-C (300V limit). Top for nominal flux, bottom for 1.5 X flux. Both for T(cool)=-15˚C. Ratios are plotted only for the operational periods.

4.3 Operation parameters

A standard plot with various operation parameters (Voltage, Temperature, Total power in Si bulk, Total leak current and Maximum strip current) is made for each set of environmental conditions. Only representative plots are shown as follows;

Fluence	Radius	T(cool) = -10˚C		T(cool) = -15˚C	
		nose	coverall	nose	coverall
nominal	300 mm	Figure 13	Figure 14	Figure 15	Figure 16
	520 mm	Figure 21	------	------	------
1.5 × nominal	300 mm	Figure 17	Figure 18	Figure 19	Figure 20
	520 mm	Figure 22	------	------	------

Summaries of the thermal profile are shown in Figure 10 for -10˚C and Figure 11 for -15˚C both at 1.5 X nominal fluence. One can see survivability of the detector system from these figures.

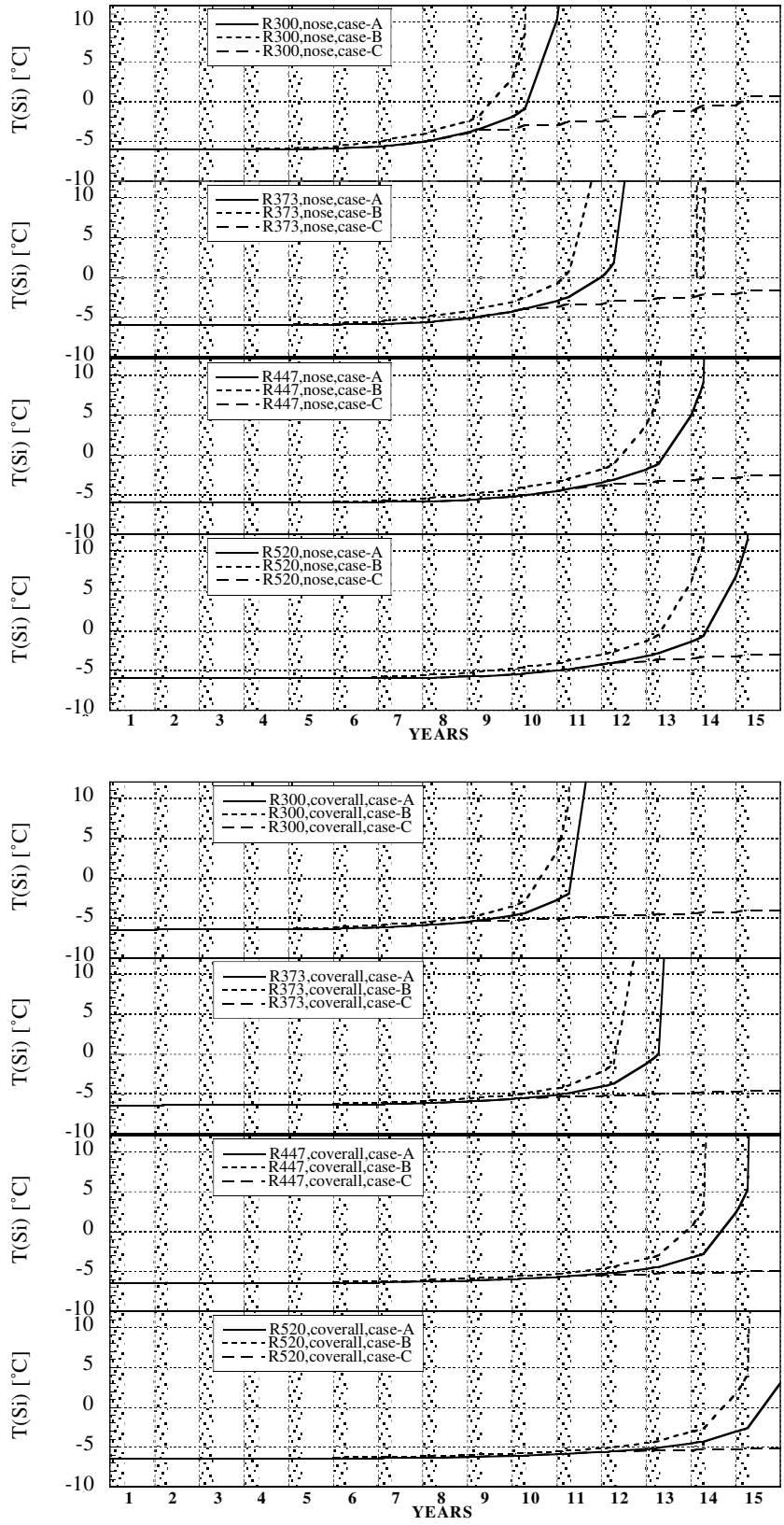

Figure 10 Yearly profile of detector temperature (left-top corner) for 1.5 X nominal fluence and T(cool)=-10˚C. Top graphs are for the module type “nose” and bottom for “coverall”.

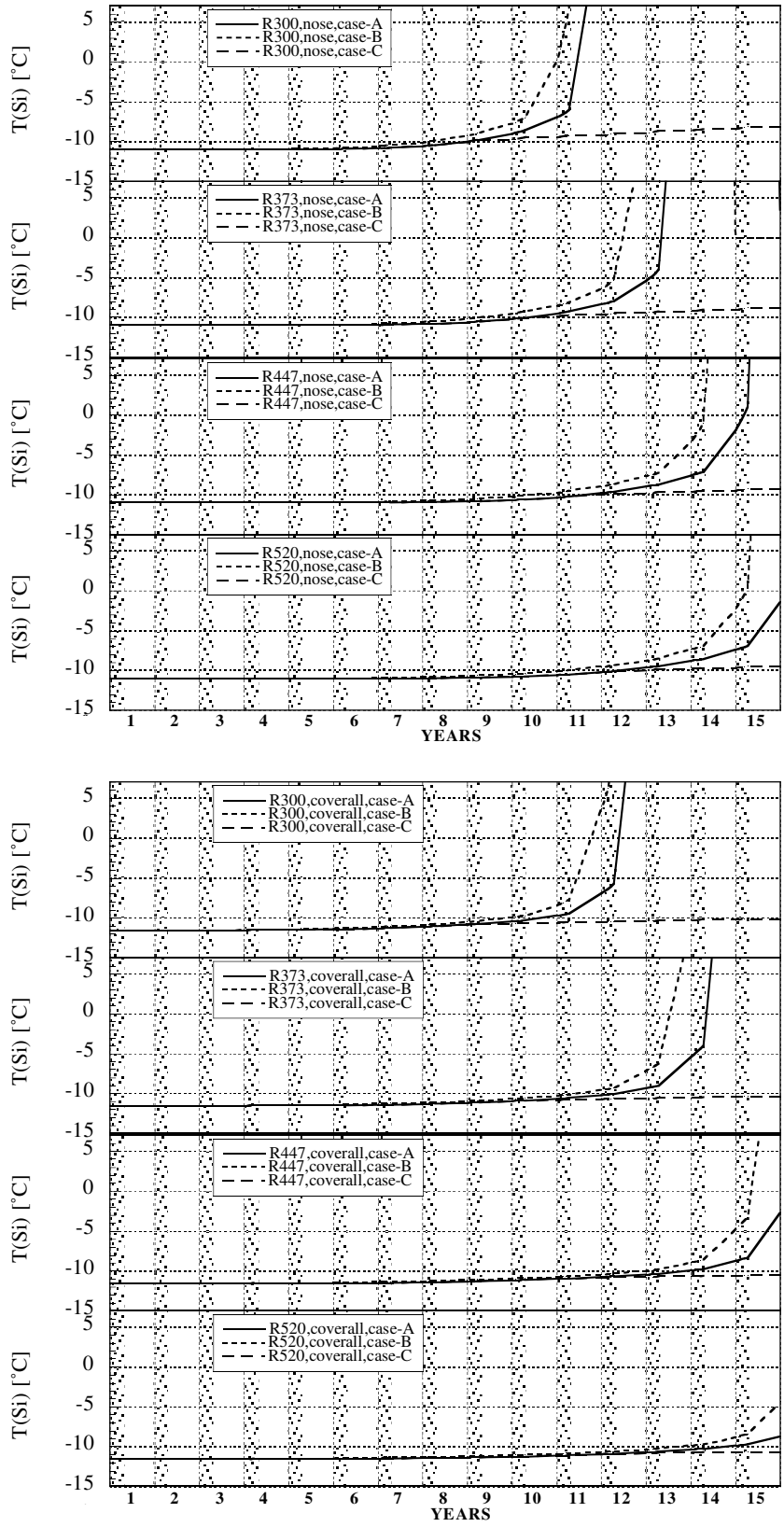

Figure 11 Yearly profile of detector temperature (left-top corner) for 1.5 X nominal fluence and T(cool)=-15˚C. Top graphs are for the module type “nose” and bottom for type “coverall”.

4.4 Life of the detector unit

Now we are going to apply two operation limits to these yearly profile to get operation periods. The criteria used to determine the operation life are

V-limit : V(apply) ≤ 500 V for Cases A and B, V(apply)/V(dep) ≥ 0.70 for Case C,

T-limit : Temperature of the left-top corner ≤ 0˚C.

These two limits are regarded as "critical" limits on detector operation, while other operational parameters such as total heat generation (Qsi), total leak current (Isi) and strip current (Istrip) are considered to be not fatal in the detector operation in this study.

The maximum applied voltage is set at 500 V since there are little experience of operation above this value. In addition, the bulk leakage current seems to rise rapidly at around 500 V as indicated in Figure 2. For Case-C (n-on-n), the ratio V(apply)/V(dep) is required to be above 0.70 for decent charge collection. It is set to 0.70 instead of 0.5 to absorb the uncertainty in the V(dep) prediction (just like Case-B in which V(apply) is set to 100 V above V(dep) to accommodate the possible V(dep) uncertainty).

The T-limit (temperature limit) is set to 0˚C because all the temperature profiles as a function of year show fairly rapid increases to thermal runaway points once it reaches at 0˚C.

Table 3 is the summary of the operational years (=life) of the detector unit obtained by applying the above operational criteria. In the table, for example, life "12 E" means the corresponding criterion is violated in between 12-th and 13-th operational year. life "11.5" indicates the criterion is violated during the 11-th year operation. Two lives (V-limit life and T-limit life) are shown in each case.

Table 3 Operation period (life) in unit of operating years. Column V-limit shows the life due to the voltage limitation and column T-limit shows the life due to thermal limitation. In the table, life "12 E" means the corresponding criterion is violated in between 12-th and 13-th operational year. life "11.5" indicates the criterion is violated during the 11-th year operation.

radius (mm)	V(appl) scenario	Nominal Fluence						1.5 X Nominal Fluence					
		T(cool) = -10˚C			T(cool) = -15˚C			T(cool) = -10˚C			T(cool) = -15˚C		
		V-Limit	T-Limit		V-Limit	T-Limit		V-Limit	T-Limit		V-Limit	T-Limit	
			nose	coverall		nose	coverall		nose	coverall		nose	coverall
300	case A	13E	13E	14E	14E	14E	15E	10E	10E	11E	11E	11E	12E
	case B	12E	12E	13E	12E	14.5	15E	10E	9E	10E	10E	10E	11E
	case C	13E	≥16	≥16	13E	≥16	≥16	10E	15.5	≥16	10E	≥16	≥16
373	case A	15E	15E	≥16	≥16	≥16	≥16	12E	11E	13E	12E	13E	14E
	case B	14E	14E	15E	14E	≥16	≥16	11E	11.5	12E	11E	12E	13E
	case C	15E	≥16	≥16	15E	≥16	≥16	12E	≥16	≥16	12E	≥16	≥16
447	case A	≥16	≥16	≥16	≥16	≥16	≥16	14E	13E	14E	14E	15E	≥16
	case B	≥16	≥16	≥16	≥16	≥16	≥16	12E	12E	13E	12E	14E	15E
	case C	≥16	≥16	≥16	≥16	≥16	≥16	13E	≥16	≥16	13E	≥16	≥16
520	case A	≥16	≥ 16	≥16	≥16	≥16	≥16	14E	14E	15E	15E	≥16	≥16
	case B	≥16	≥ 16	≥16	≥16	≥16	≥16	13E	13E	14E	13E	15.5	≥16
	case C	≥16	≥ 16	≥16	≥16	≥16	≥16	14E	≥16	≥16	14E	≥16	≥16

There remain some warnings about the detector operation as high as 500 V. To evaluate the dependence on V-limit, it is changed from 300 to 500 V for the case-B (p-on-n) as shown in Table 4. Roughly speaking, each 100 V increase in V-limit extends the detector life by one or two years. It is also noted that there is very little dependence on the cooling temperature 110˚C or -15˚C.

Table 4 Dependence of life on the V-limit voltage (300, 400 and 500 V) for Case-B (p-on-n).

radius (mm)	V(appl) scenario	Nominal Fluence						1.5 X Nominal Fluence					
		-10˚C			-15˚C			-10˚C			-15˚C		
		V-limit			V-limit			V-limit			V-limit		
		300 V	400 V	500 V	300 V	400 V	500 V	300 V	400 V	500 V	300 V	400 V	500 V
300	case B	9E	11E	12E	9E	11E	12E	7E	8E	10E	7E	8E	10E
373	case B	11E	13E	14E	11E	13E	14E	8E	10E	11E	8E	10E	11E
447	case B	12E	14E	≥16	12E	14E	≥16	9E	11E	12E	9E	11E	13E
520	case B	13E	15E	≥16	13E	15E	≥16	10E	12E	13E	10E	12E	13E

"Combined life" is defined to be the shorter one of the two lives. Figure 12 shows graphically the combined lives of the cases B and C.

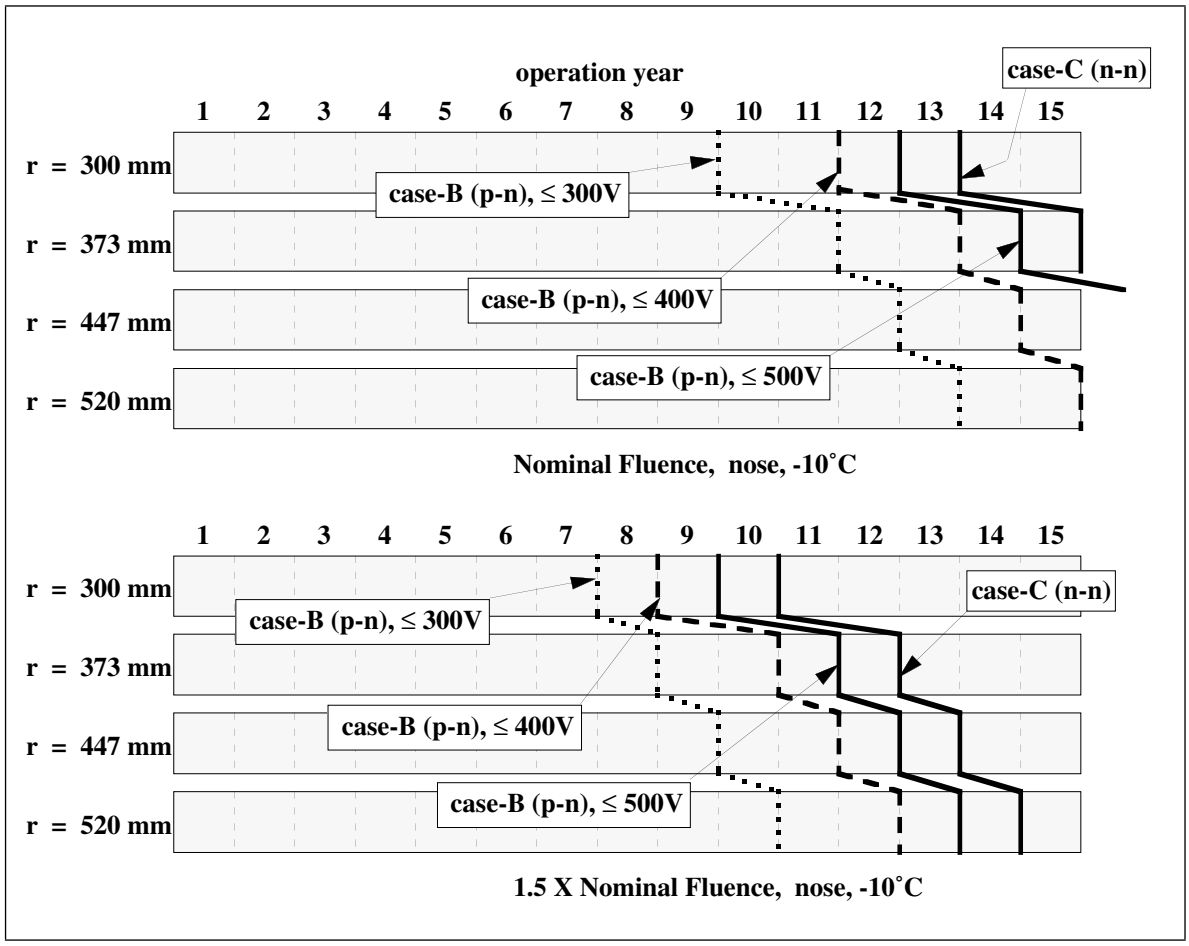

Figure 12 Combined lives of the SCT detector at various radii for nominal (top) and 1.5 X nominal (bottom) fluence. Module type: nose. T(cool)=-10˚C.

5. Points of observation

1. The depletion voltage increases non-linearly due to the increasing contribution by the anti-annealing term in later years [Figures 7 and 8].

2. The evolution of depletion voltage shows little difference for two cooling (actually contact) temperatures T(cool) of -10˚C and -15˚C [Figure 8]. This is because almost all the anti-annealing part is increased by the warm-up during the access periods [Figure 7].

3. Two fluence scenarios (nominal and 1.5 X nominal) generate a large difference in deple-

tion voltage prediction [Figure 8]. For example, at r=300mm and after 10-th year operation, the predicted depletion voltage is ~200 V for nominal fluence as opposed to ~400 V for 1.5 X nominal one.

4. The yearly profile of detector temperature shows rather flat and stable behavior except last one or two years before its catastrophic end of thermal runaway [Figures 10 and 11]. This somewhat unexpected profile can be qualitatively explained by the multiplicative combination of three evolutions: (1) non-linear growth of depletion voltage (and applied voltage), (2) increase of leakage current as applied voltage [Figure 2], and (3) non-linear response of detector temperature [Figure 5].

5. The operation life of the detector unit is in general determined by the voltage limit (V-limit) rather than the thermal limit (T-limit) [Table 3]. Especially in Case-C (n-on-n like), the voltage limit $R_V \geq 0.70$ is violated many years before the year of thermal limit. This is a natural consequence of its restriction of V(apply) ≤ 300 V. In Case-A and -B (p-on-n like), however, the thermal and voltage limits occur in the similar year range. Thus one can empirically say "500V limit ~ thermal limit" for the module type nose.

6. Thermally stronger module type "coverall" extends the thermal-limit life by one year [Table 3]. One can also extend the thermal life one more year by lowering the cooling temperature from -10˚C to -15˚C [Table 3].

7. The life strongly depends on the detector radius. There are generally two-year differences between the lives of ring-1 (r=300 mm) and ring-2 (373 mm), and one year step each beyond [Table 3 & Figure 12]. So the ring-1 dominates the life of the detector system.

8. The value of V-limit strongly affects the overall life of the detector unit. The limit change from 500 V to 300 V will shorten the life by about 3 years in Case-B (p-on-n like) [Table 4 & Figure 12]. Therefore the capability of HV operation up to 500 V is important for long life.

9. Optimization

Based on the several points listed above, it becomes clear that the voltage to be applied on detectors is the main and key limiting factor for the life of detector operation. In the case of p-on-n detectors, the strong dependence of the life on the maximum applied voltage indicates a need of stable operation in the range of 300 to 500 V.

If the stable operation of such a HV range is not guaranteed, it is recommended to use n-on-n type detectors for long life of operation. The strong dependence of life on the detector radius suggests that a optimum solution for longest possible life of the system operation is

- to use n-on-n type for inner one or two rings, and
- to employ p-on-n detectors in outer regions of radius.

This combination avoids the detector operation at higher voltage range near 500 V, while it extends the operation life at smaller radii.

For example, if 400 V operation is reachable as a reasonable guess, the operational life of the combination of n-on-n for ring-1 and p-on-n for rings 2-4 will be 10, 10,11 and 12 years for rings 1,2,3 and 4, respectively, even for the case of 1.5 X nominal fluence case (see Figure 12).

Operation at lower temperature or use of thermally stronger module type will extend the life by another one or two (but not more) years. Application of these improvements on inner rings is also recommended.

10. Summary

The operation of the ATLAS barrel silicon microstrip detector is predicted under the various external conditions;

- nonimal fluence and1.5 X niminal fluence,
- detector locations at r = 300, 373, 447 and 520 mm,
- cooling contact temperature at -10˚C ans -15˚C,
- two barrel module types “nose” and “coverall”,
- standard access scenario of 2 days at 20˚C and 14 days at 17˚C,
- three scenarios of the applied voltage V(apply);

case-A:	V(apply) ≥ V(dep),
case-B (p-on-n):	V(apply) = V(dep) + 100 V ,
case-C (n-on-n):	V(apply) ≥ V(dep) but V(apply) ≤ 300 V,

Identical set of the evolution parameters as described in TDR is used except an additional term for short-time annealing. To evaluate the power generation in the bulk, the voltage dependence of the leak current recently measured is used. Results from thermal model simulation are also used to predict the thermal behavior of the module.

The study has revealed number of interesting observation such as

- non-linear increase of depletion voltage in later years,
- little difference in depletion voltage at -10˚C and -15˚C operation,
- stable thermal behavior up to the last 1~2 years of operation,
- the voltage limit as a main reason for life,
- one year extension of life by coverall type and/or -15˚C operation,
- strong dependence of life on detector radius,
- strong dependence of life on maximum attainable volatge in case of p-on-n type.

Based on these observations, the author recommends a combined configuration of detector types as an optimum solution including a safety margin for detector operation.

References

[1] ATLAS Inner Detector Technical Design Report, CERN/LHCC/97-17, 30 April, 1997.

[2] H. -J. Ziock et al., Nucl. Instr. and Meth. A342 (1995) 96, E. Fretwurst et al., Nucl. Instr. and Meth. A342 (1994) 119, and A. Chilingarov et al., Nucl. Instr. and Meth. A360 (1995) 423.

[3] J. Matthews et al., ATLAS Internal Note, INDET-NO-118, 12 Dec. 1995.

[4] C. Buttar and J. Carter, private communication, Nov. 1997.

[5] recommended by T. Ohsugi and H.F-W. Sadrozinski.

–

_____

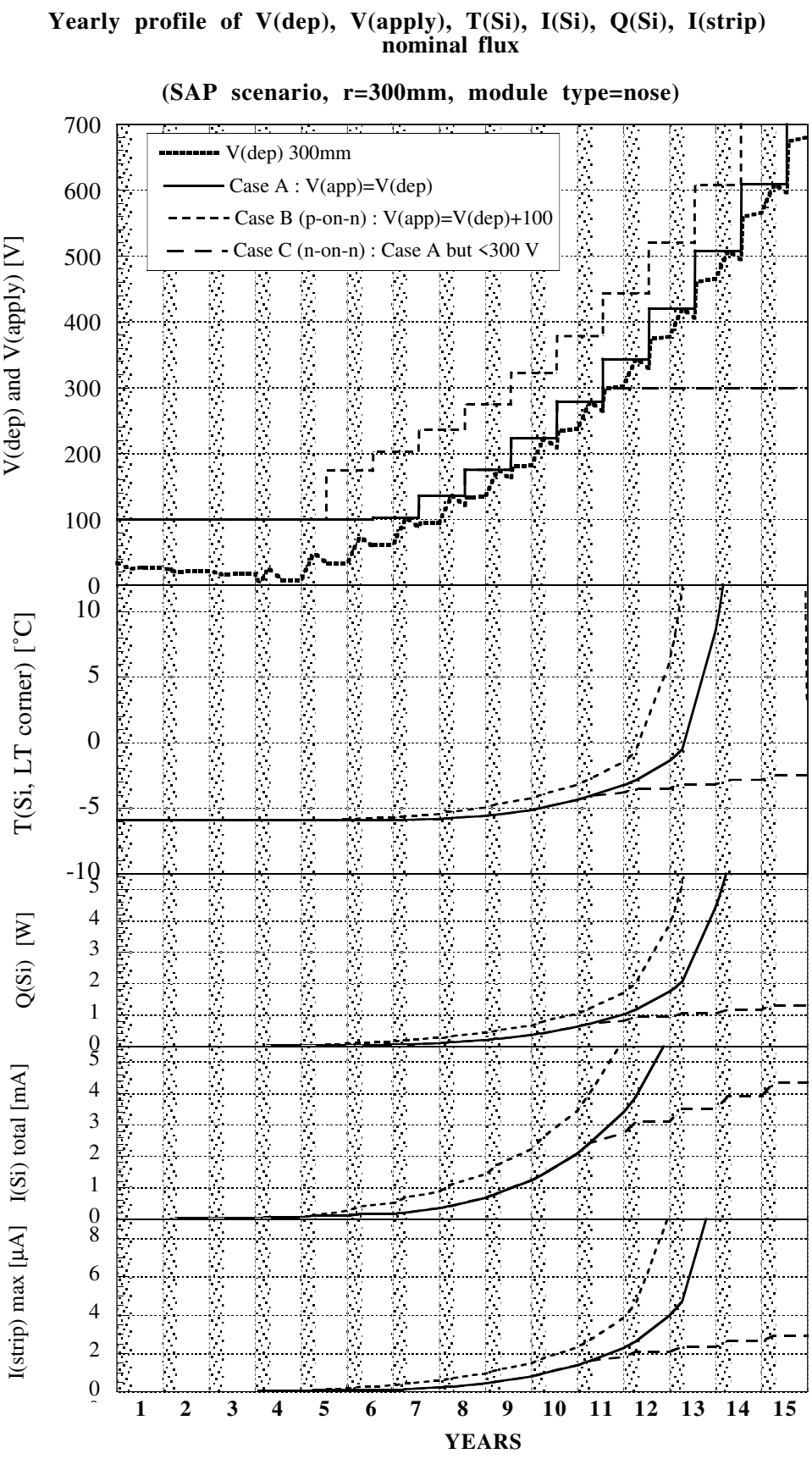

Figure 13 Operation at nominal fluence, r=300 mm, module type = nose, contact temperature at -10 ˚C.

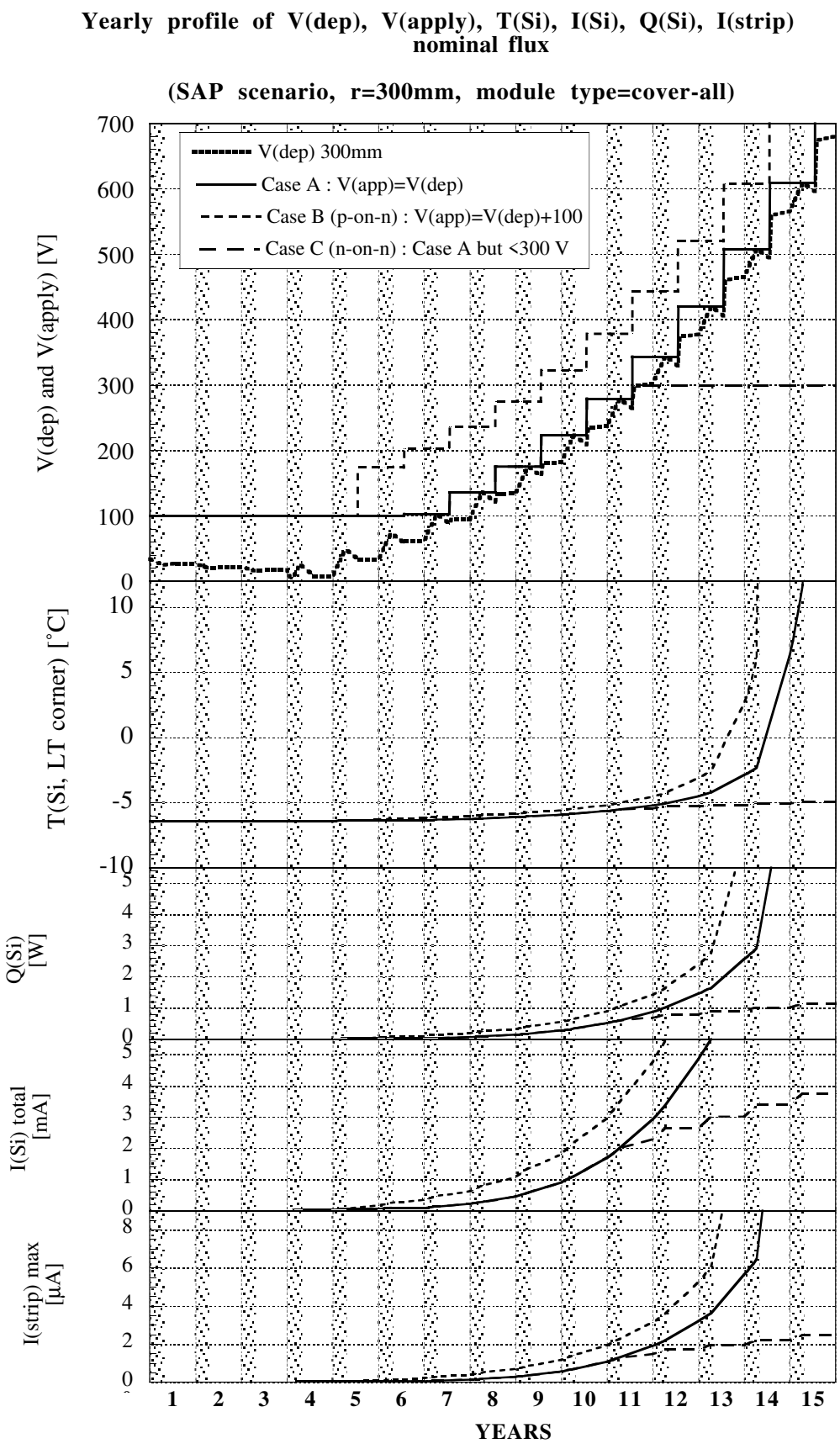

Figure 14 Operation at nominal fluence, r=300 mm, module type = coverall, contact temperature at -10 ˚C.

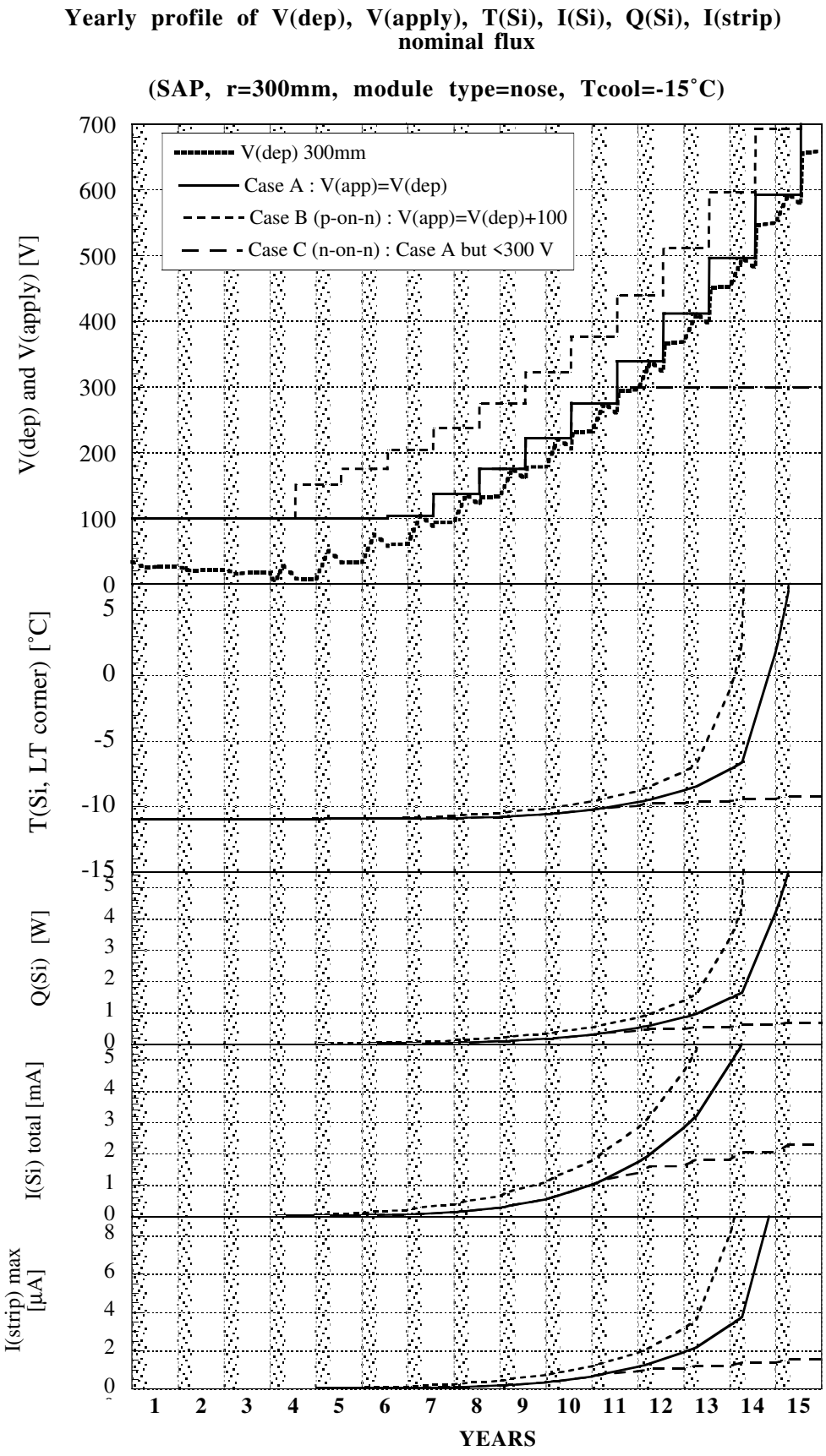

Figure 15 Operation at nominal fluence, r=300 mm, module type = nose, contact temperature at -15 ˚C.

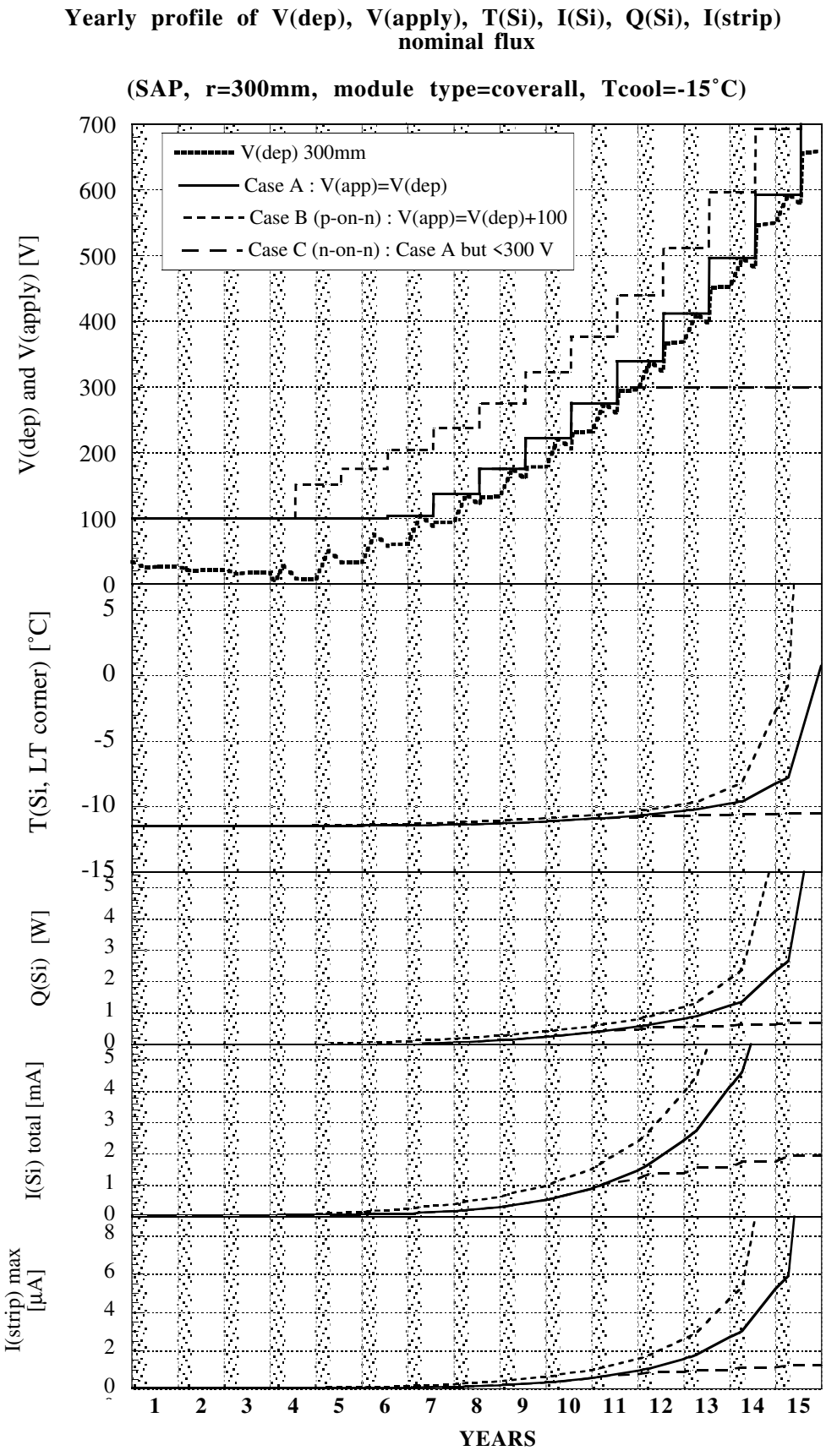

Figure 16 Operation at nominal fluence, r=300 mm, module type = coverall, contact temperature at -15 ˚C.

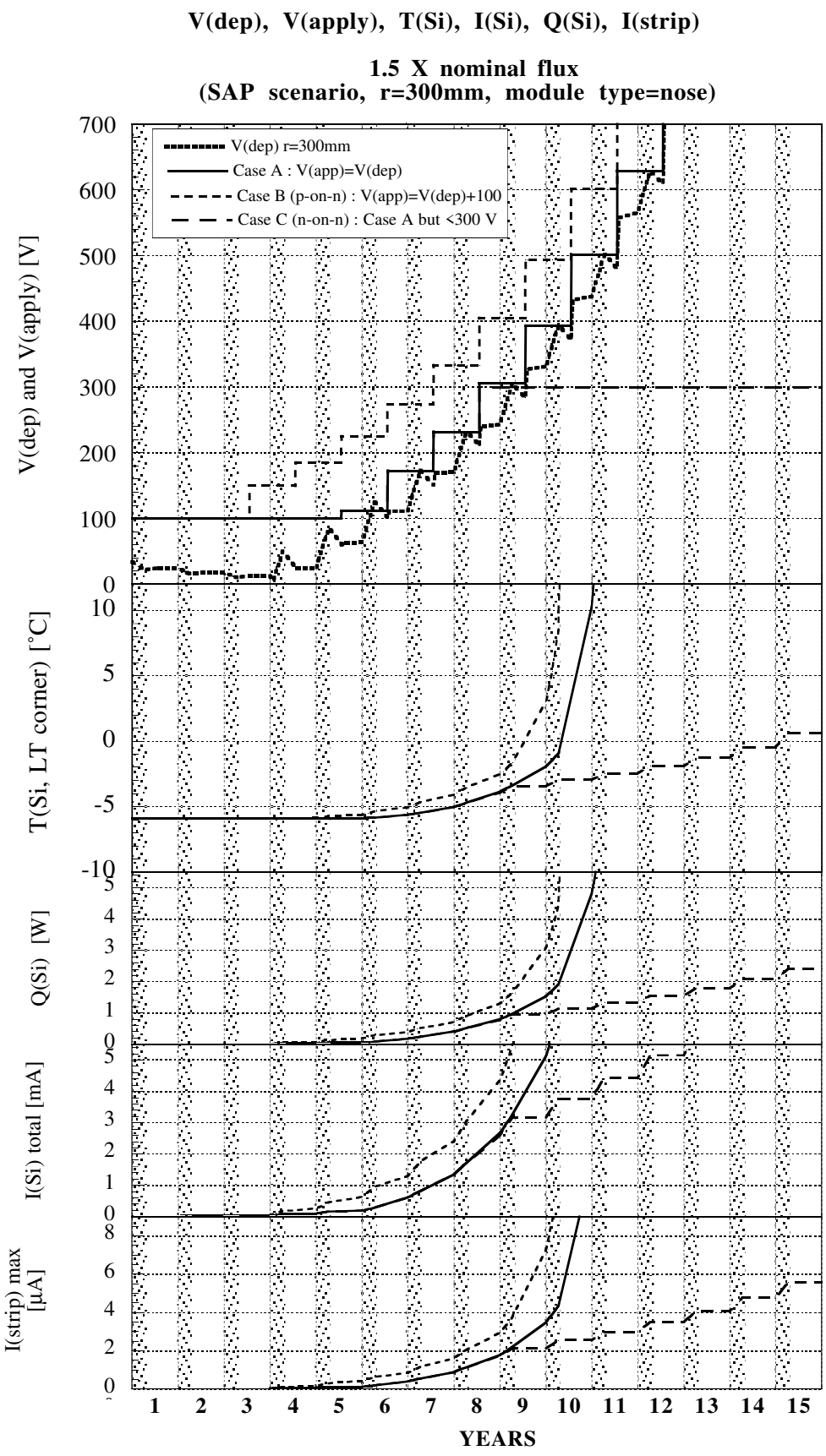

Figure 17 Operation at 1.5 X nominal fluence, r=300 mm, module type = nose, contact temperature at -10 ˚C.

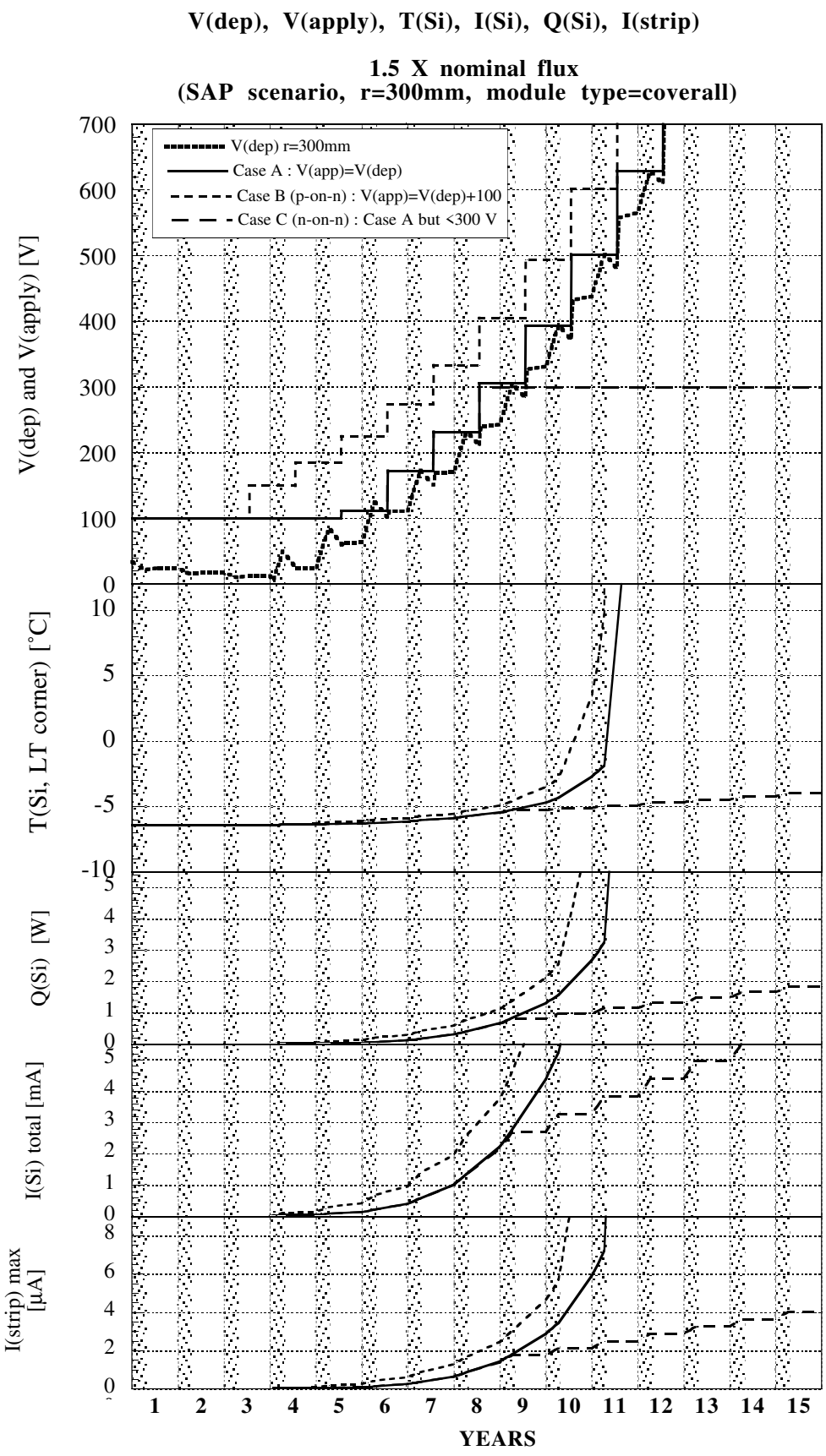

Figure 18 Operation at 1.5 X nominal fluence, r=300 mm, module type = coverall, contact temperature at -10 ˚C.

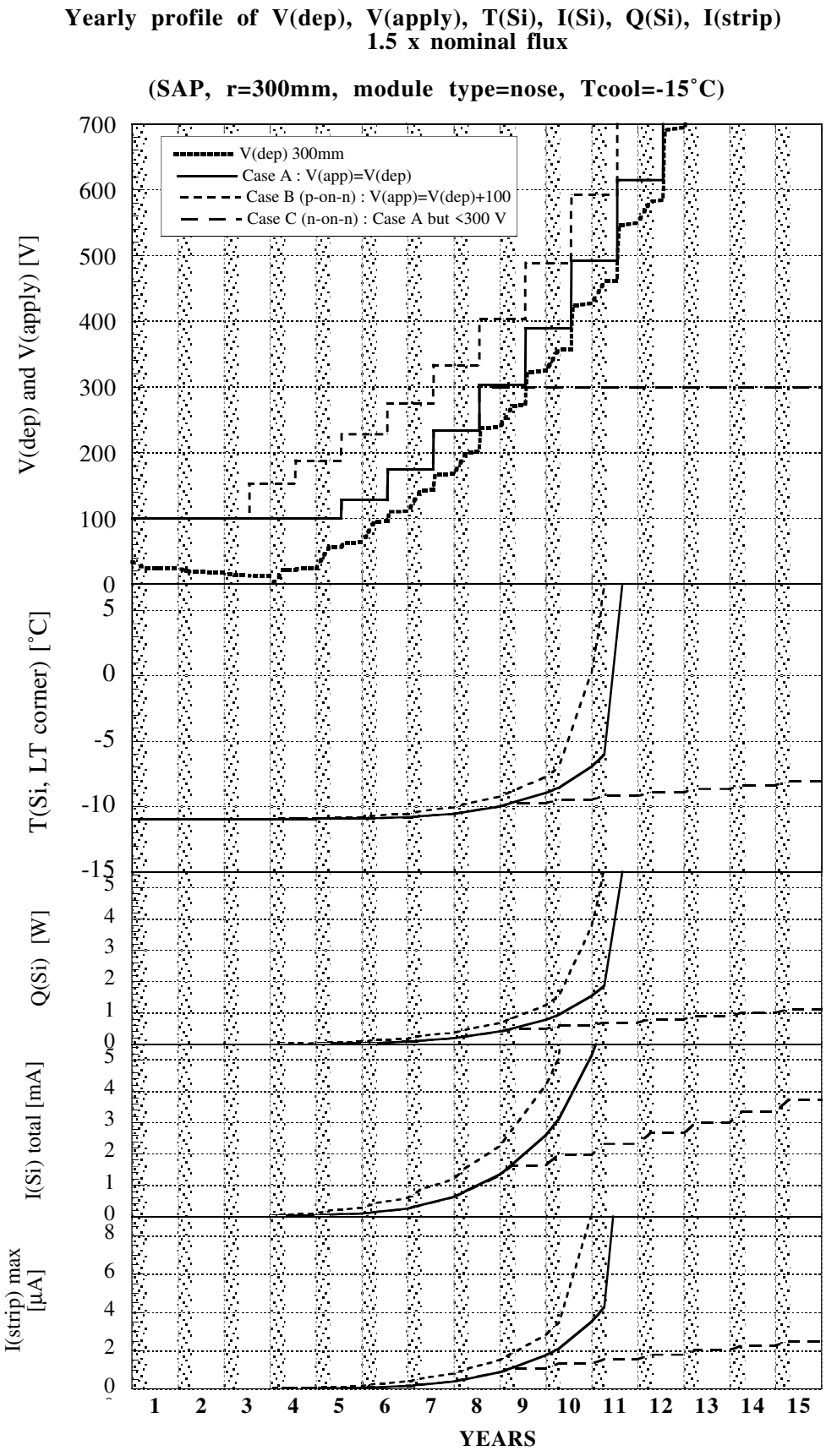

Figure 19 Operation at 1.5 X nominal fluence, r=300 mm, module type = nose, contact temperature at -15 ˚C.

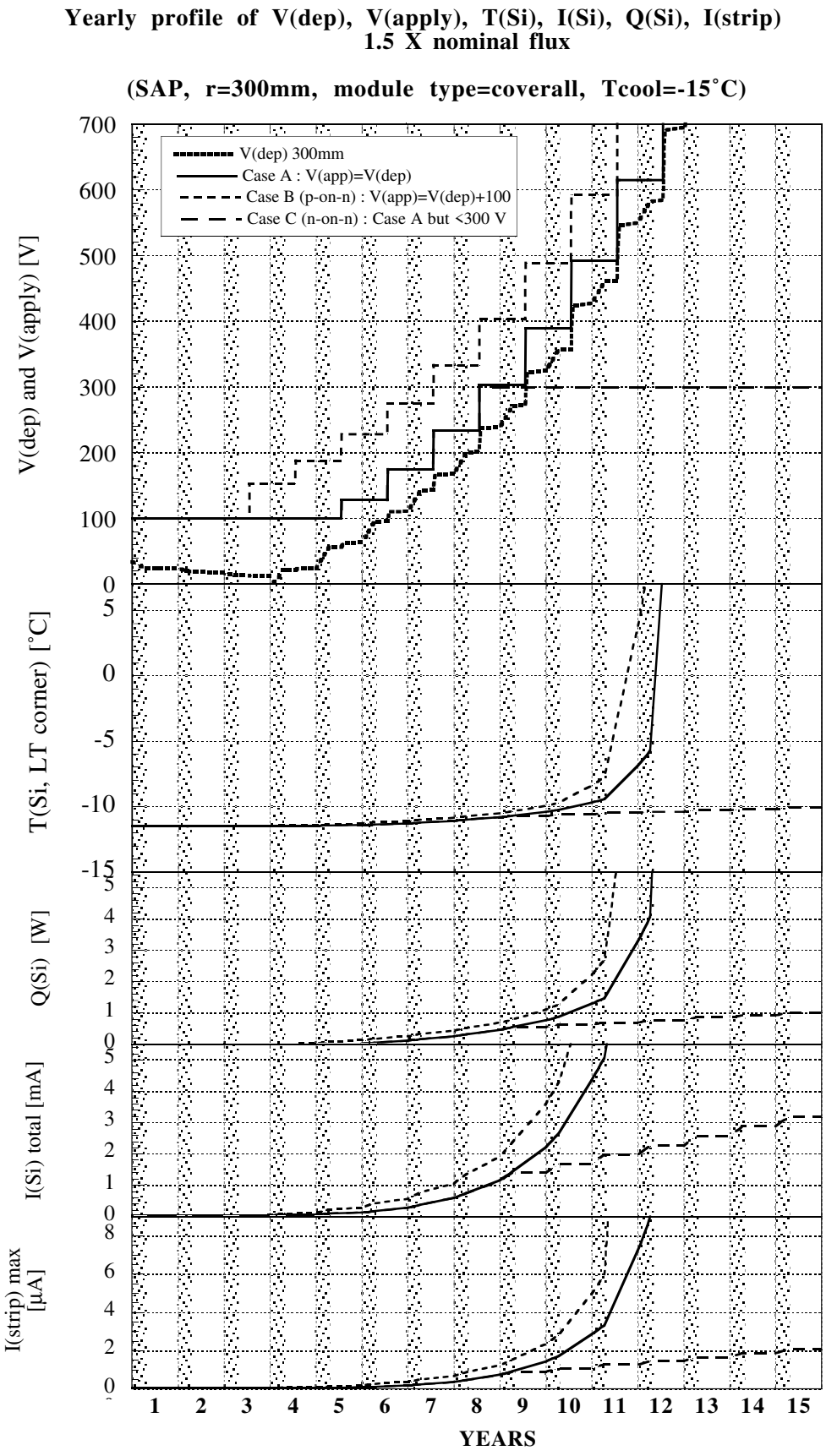

Figure 20 Operation at 1.5 X nominal fluence, r=300 mm, module type = coverall, contact temperature at -15 ˚C.

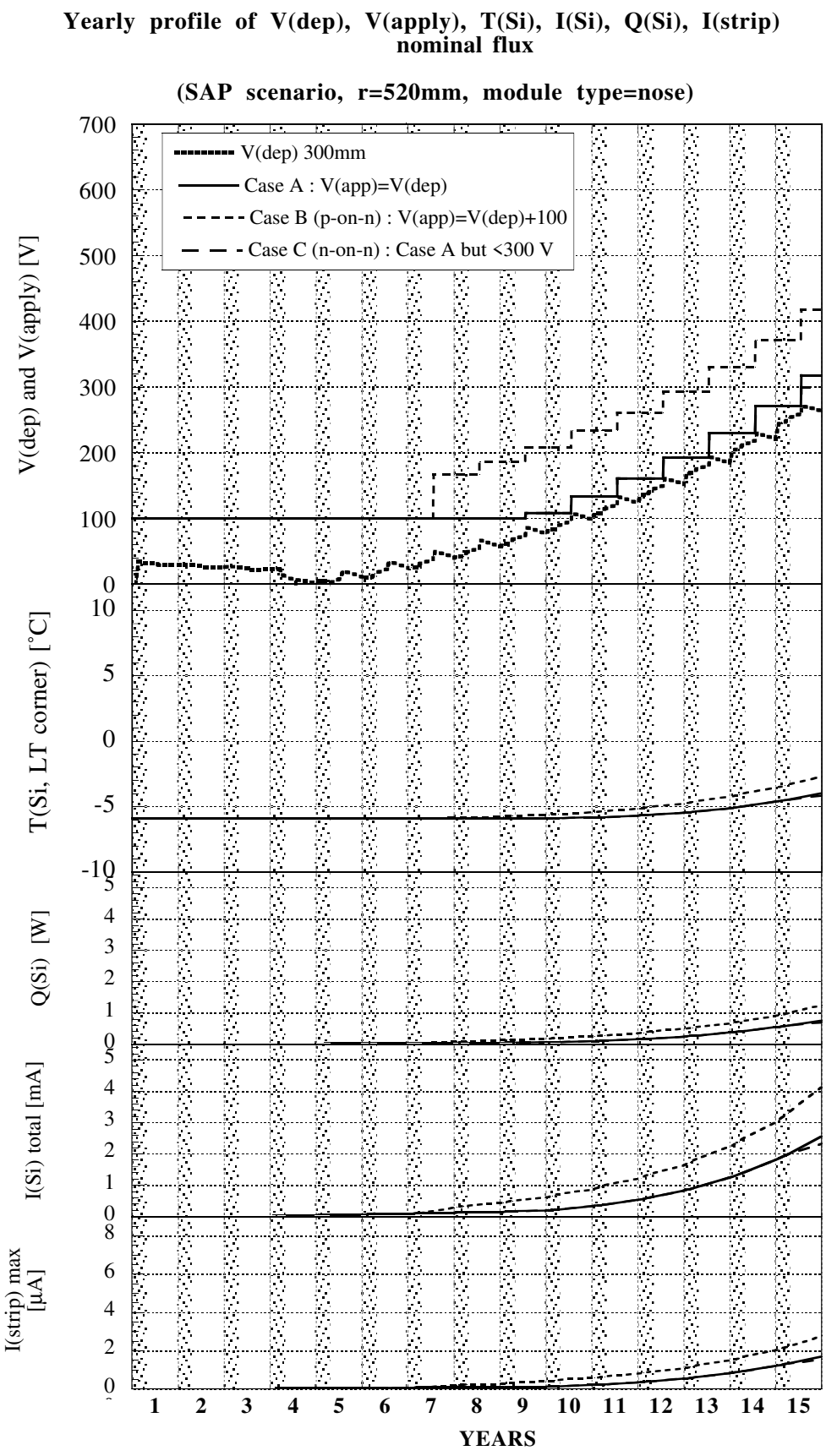

Figure 21 Operation at nominal fluence, r=520 mm, module type = nose, contact temperature at -10 ˚C.

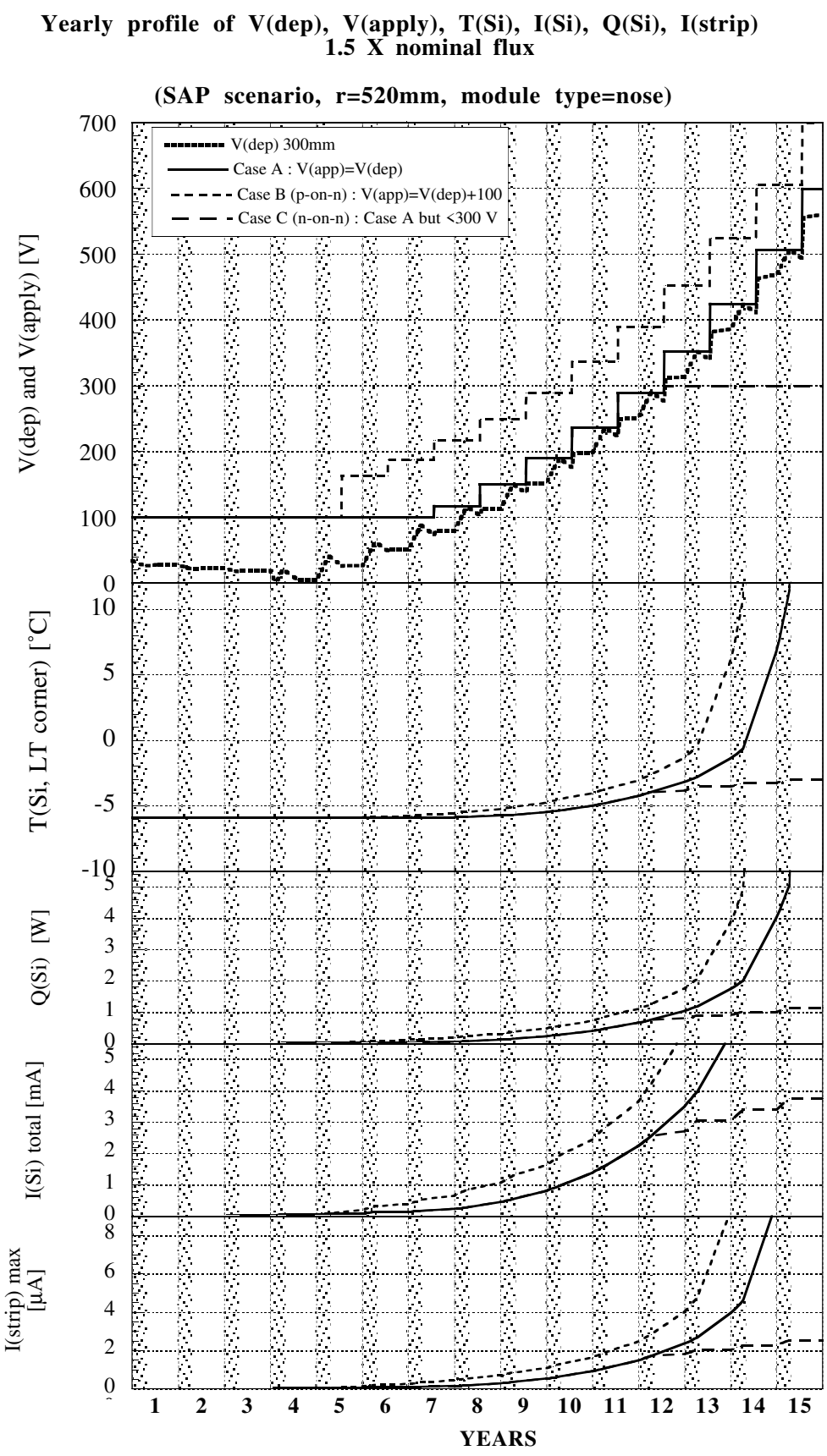

Figure 22 Operation at 1.5 X nominal fluence, r=520 mm, module type = nose, contact temperature at -10 ˚C.